CI&CEQ

Available on line at
Association of the Chemical Engineers of Serbia AChE
www.ache.org.rs/CICEQ

Chemical Industry & Chemical Engineering Quarterly 19 (3) 369–375 (2013) CI&CEQ

JELENA Đ. MARKOVIĆ
NATAŠA LJ. LUKIĆ
ALEKSANDAR I. JOKIĆ
BOJANA B. IKONIĆ
JELENA D. ILIĆ
BRANISLAVA G. NIKOLOVSKI

University of Novi Sad, Faculty of Technology, Novi Sad, Serbia

SCIENTIFIC PAPER

UDC 66.045.1:66.06:5/.6

DOI 10.2298/CICEQ120309071M

2D SIMULATION AND ANALYSIS OF FLUID FLOW BETWEEN TWO SINUSOIDAL PARALLEL PLATES USING LATTICE BOLTZMANN METHOD

In order to obtain better heat transfer, it is important to enhance fluid mixing in heat exchangers. Since there are negative effects when heat exchangers are operating in the turbulent regime (such as significant pressure drop and increased size of the pump), it is necessary to apply techniques that would provide better fluid mixing when heat exchangers are operating in the laminar regime. Investigations have shown that the use of sinusoidal instead of flat plates results in this effect. This study is a result of two-dimensional simulation of fluid flow between two parallel sinusoidal plates. Simulation was done with the use of modified OpenLB code, based on the lattice Boltzmann method. The Reynolds number was varied from 200 to 1000, and the space between the plates was varied from 3 to 5 cm. The results showed that sinusoidal plates enhance fluid mixing, especially with greater values of Re and smaller space between the plates, which is in agreement with previous investigations.

Keywords: lattice Boltzmann, fluid flow, sinusoidal plates, plate heat exchanger, simulation.

In heat exchanger design it is very important to obtain good fluid mixing, reduce heat transfer resistance, and minimize pressure drop. Good fluid mixing can be obtained in heat exchangers working in the turbulent regime, which, on the other hand, has a significant pressure drop as a negative effect. When operating in the turbulent regime, the pumping cost increases as the size of the pump increases, which is often a limiting factor, especially in compact heat exchangers or in heat exchangers with very viscous fluids. Enhancement of fluid mixing in laminar regime, which leads to better heat transfer, is possible to obtain when chaotic fluid flow is established. Chaotic advection occurs when pathlines that do not conform to laminar regime are present in the fluid, and can be generated in ducts with periodically perturbed geometry in downstream direction.

In order to obtain better heat transfer in plate heat exchangers, several techniques have been used so far. One of the most often applied techniques was the use of wavy plates instead of flat plates [1], and many investigations showed that use of sinusoidal instead of flat plates enhances heat transfer without significant pressure drop [2-7].

The aim of this study was to simulate and analyze the fluid flow between two parallel sinusoidal plates with the use of the lattice Boltzmann method (LBM). In recent years, LBM has developed into an alternative and promising numerical scheme for simulating fluid flows and modeling physics in fluids. Unlike conventional numerical schemes based on discretizations of macroscopic continuum equations, the LBM is based on microscopic and mesoscopic kinetic equations.

THEORETICAL PART

Lattice Boltzmann Method

The fundamental idea of the LBM is to construct simplified kinetic models that incorporate the essential physics of microscopic or mesoscopic processes so that the macroscopic averaged properties obey the desired macroscopic equations. Even though it is based on a particle picture, its principal focus is the averaged macroscopic behavior. The kinetic equation

Correspondence: J.Đ. Marković, University of Novi Sad, Faculty of Technology, Bulevar cara Lazara 1, 21000 Novi Sad, Serbia.
E-mail: jmarkovic@tf.uns.ac.rs
Paper received: 9 March, 2012
Paper revised: 27 June, 2012
Paper accepted: 4 July, 2012

provides many of the advantages of molecular dynamics, including clear physical pictures, easy implementation of boundary conditions, and fully parallel algorithms. Because of the availability of very fast and massively parallel machines, there is a current trend to use the code that can exploit the intrinsic features of parallelism. The LBM fulfills these requirements in a straightforward manner.

The kinetic nature of the LBM introduces three important features that distinguish it from other numerical methods. First, the convection operator (or streaming process) of the LBM in phase space (velocity space) is linear. The feature is borrowed from kinetic theory, and contrasts with the nonlinear convection terms in other approaches that use a macroscopic representations. Simple convection combined with a relaxation process (or collision operator) allows the recovery of the nonlinear macroscopic advection trough multi-scale expansions. Second, the incompressible Navier-Stokes (NS) equations can be obtained in the nearly incompressible limit of the LBM. The pressure of the LBM is calculated using **n** equations of state. In contrast, in the direct numerical simulation of the incompressible NS equations, the pressure satisfies a Poisson equation with velocity strains acting as sources. Solving this equation for the pressure often produces numerical difficulties requiring special treatment, such as iteration or relaxation. Third, the LBM utilizes a minimal set of velocities in phase space. In the traditional kinetic theory with the Maxwell-Boltzmann equilibrium distribution, the phase space is a complete functional space. The averaging process involves information from the whole velocity phase space. Because only two speeds and only a few moving directions are used in LBM, the transformation relating the microscopic distribution function and macroscopic quantities is greatly simplified.

The LBM originated from lattice gas (LG) automata, a discrete particle kinetics utilizing a discrete lattice and discrete time, which consists of a regular lattice with particles residing on the nodes. A set of Boolean variables $n_i(x,t)$ (i = 0,…,M) describing the particle occupation is defined, where M is the number of directions of the particle velocities at each node. The evolution equation of the LG automata is as follows:

$$n_i(x+e_i,t+1) = n_i(x,t) + \Omega(n(x,t)),\ i = 0,1\ldots,M \qquad (1)$$

where e_i are local particle velocities starting from an initial state. The configuration of particles at each time step evolves in two sequential sub-steps: a) streaming, in which each particle moves to the nearest node in the direction of its velocity and b) collision, which occurs when particles arriving at a node interact and change their velocity directions according to scattering rules. For simplicity, the exclusion principle (no more than one particle being allowed at a given time and node with a given velocity) is imposed for memory efficiency and leads to a Fermi-Dirac local equilibrium distribution.

The main feature of the LBM is to replace the particle occupation variables, n_i (Boolean variables), in Eq. (1) by single-particle distribution functions (real variables), $f_i\langle n_i\rangle$, and neglect individual particle motion and particle-particle correlations in the kinetic equations, where $\langle\rangle$ denotes an ensemble average. An important simplification of the LBM was made by linearization of the collision operator by assuming that the distribution is close to the local equilibrium state. An enhanced collision operator approach which is linearly stable was proposed [10]. A particular linearized version of the collision operator makes use of relaxation time towards the local equilibrium using a single time relaxation. The relaxation term is known as the Bhathnagar-Gross-Krook (BGK) collision operator and has been independently suggested by several authors [11,12]. In this lattice BGK model (LBGK), the local equilibrium distribution is chosen to recover the Navier-Stokes macroscopic equations. Use of LBGK model makes the computations more efficient and allows flexibility of the transport coefficients [13] .

Lattice Botlzmann equations

The lattice Boltzmann equation (LBE) is an explicit time-marching finite-difference representation of the continuous Boltzmann equation in phase space and time. The LBE incorporating the single relaxation BGK approximation has the form [11]:

$$f_i(x+c_i\Delta t, t+\Delta t) - f_i(x,t) = \omega[f_i^{\mathrm{eq}}(x,t) - f_i(x,t)] \qquad (2)$$

where $\omega \equiv \Delta t/\tau$ denotes the relaxation factor with limits $0 < \omega < 2$, $c_s = c/\sqrt{3}$ is the speed of sound, and $c = \Delta x/\Delta t$. The kinematic viscosity is given by the relaxation factor:

$$\nu = (2/\omega - 1)\Delta x c/6 \qquad (3)$$

The local equilibrium distribution is an analog version of the Maxwellian distribution function for incompressible flows, and is expressed as:

$$f_i^{\mathrm{eq}}(x,t) = w_i\rho[1 + \frac{c_{i\mathrm{A}}u_{\mathrm{A}}}{c_s^2} + \frac{u_{\mathrm{A}}u_{\mathrm{B}}}{2c_s^2}(\frac{c_{i\mathrm{A}}c_{i\mathrm{B}}}{c_s^2} - \delta_{\mathrm{AB}})] \qquad (4)$$

In these expressions, the flow properties are defined as:

Flow density: $\rho = \sum_i f_i$ (5)

Momentum: $\rho u_A = \sum_{iA} f_i c_{iA}$ (6)

In the equations above, sub-indices A and B denote the components of the Cartesian coordinates with implied summation for repeated indices. Furthermore, w_i is the weighting which can be determined to achieve isotropy of the fourth-order tensor of velocities and Galilean invariance [11]. Applying the Chapman-Enskog expansion, the continuity equation and the Navier-Stokes equations can be recovered exactly at the second order approximation from the LBE if the density variation is sufficiently small [14].

For the D2Q9 (two-dimensional nine velocities) models, the weightings in Eq. (4) are assigned as follows: $w_i = 4/9$ for $|c_i| = 0$ (*i.e.*, static particle), $w_i = 1/9$ for $|c_i| = 1$, and $w_i = 1/36$ for $|c_i| = \sqrt{2}$. The lattice Boltzmann method applies two essential steps, namely collision and propagation, to reveal the flow phenomena at the mesoscopic scale. Hence, the corresponding computations of LBM are performed as:

Collision step:

$$\tilde{f}_i(x,t) = f_i(x,t) + \omega[f_i^{eq}(x,t) - f(x,t)] \quad (7)$$

Propagation step:

$$f_i(x + c_i\Delta t, t + \Delta t) = \tilde{f}_i(x,t) \quad (8)$$

where $\tilde{f}_i$ denotes the post-collision state of the distribution function. From Eqs. (7) and (8), it is clear that the collision process is fully local and the propagation of the distribution functions is uniform. As a result, the lattice BGK scheme is very simple when applied with the unity lattice size (*i.e.*, $\Delta x = \Delta y = 1$), and a relative time step of $\Delta t = 1$ such that $c = \Delta x / \Delta t = 1$ [15].

Boundary conditions

The simulation was done with modified OpenLB LBM code with the use of bounce back boundary conditions.

To generate the solid boundary of an obstacle, links between neighbouring nodes are selected to best confirm to the shape of the obstacle. The nodes just outside the boundary no longer communicate with their neighbours inside the obstacle. Instead, a particle striking this boundary bounces back in the direction from which it arrived. The bounce-back boundary condition is known to model, to first order, a boundary which lies halfway between these boundary nodes and the neighbouring fluid nodes. It is apparent that the boundary condition cannot directly model a general curvilinear surface but instead uses a stair-step approximation of the surface.

The bounce-back condition is implemented in the lattice Boltzmann scheme after the particle distribution is updated. After the particle distribution is computed, the boundary condition reverses the direction of each component of particle distribution just inside the boundary. These components leave the boundary during the following time step.

In irregular geometries, even with the use of a staircase approximation of domain boundaries, it is quite difficult attributing the right boundary type to each cell. In this approach, particle populations that are opposite to each other are swapped at each iteration step, and no additional collision is executed. The advantage of this procedure is that it is independent of the orientation of the domain.

For the D2 Q9 scheme, the boundary conditions at the wall are given as $f_2 = f_4$, $f_5 = f_7$ and $f_6 = f_8$. f_7 is bouncing back from left hand side lattice in the solid wall and f_8 is bouncing back from the right hand lattice in the solid wall in reference to the main lattice location. f_4, f_7 and f_8 are known from the streaming process. To ensure no-slip conditions velocity at the wall is set to zero.

For low values of Re number calculations were numerically stable, but for Re > 1000, depending on the separation of the channel, in most cases it became numerically unstable [16].

Geometry of the model

The geometry of plates used in the simulation is given in Figure 1, while Eq. (9) defines the sine function used for plate geometry description.

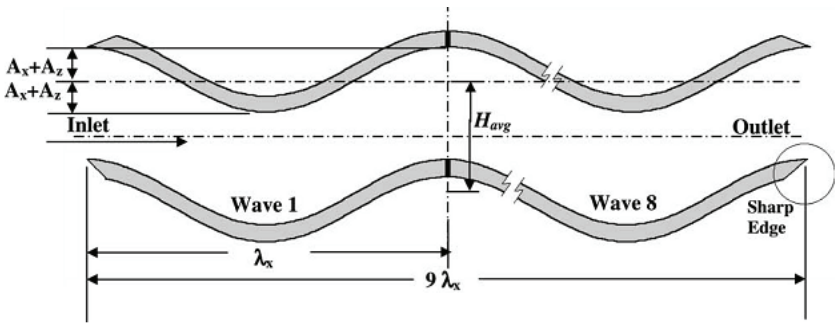

Figure.1. Geometry model of parallel plates.

$$h = A_x \sin(\frac{2\pi x}{\lambda_x}) \quad (9)$$

where h is the height of the plate at a given coordinate x, A_x wave amplitude in the x direction, and λ_x is a wavelength in the x direction. Dimensions used in the calculations are: A_x = 0.45 cm, λ_x = 8.334 cm and H_{avg} = 4 cm. The dimensionless geometric parameters that describe the corrugated plate model are given as $\lambda_x = \lambda_x / H_{avg}$ and $\beta_x = A_x / H_{avg}$, where H_{avg} is the separation between corrugated plates that form the channel, which was varied from 3 to 5 cm throughout the investigation.

The Reynolds number was defined as:

$$\mathrm{Re} = \frac{V_{in} H_{avg}}{\nu} \quad (10)$$

where V_{in} is the average velocity at the inlet of the corrugated plates and υ is the kinematic viscosity [1].

RESULTS AND DISCUSSION

The criterion used to determine if one wave has macroscopic mixing is the presence of crossing paths in the central flow, broken recirculation regions or too big vortices compared to wave amplitude. Flow mixing occurs when the core flow undergoes large oscillations, resulting in large changes in the position of the reattachment point of the free shear layer. When the reattachment point moves far enough upstream, the core flow impinging on the wall "injects" free-stream fluid into the separation bubble; this injection is accompanied by "ejection" of fluid from the separation bubble into the core flow. This dynamically driven exchange of fluid results in macroscopic mixing [6].

Low Reynolds number was set at 200, while the upper limit was 1000.

The flow pattern is very much like the one reported in previous investigations [6,17]. At small Reynolds numbers there are steady recirculation regions along the sinusoidal channel. At very low velocities (Re ≈ 200) there were no recirculation regions throughout the channel. In general, the flow moves and tries to follow the channel shape. This case is a typical Stokes flow since the viscous forces dominate the flow pattern. Steady recirculation regions could be observed in the first wave for Reynolds larger than 200. More recirculation regions are observed along the channel as the Reynolds number increases. Eventually, recirculation regions and rolling vortices appear throughout the entire channel.

Figures 2 and 3 show the flow pattern that appears in this type of channel. Recirculation regions do not cover the entire wave. As the Reynolds number and the wavelength from the channel inlet increase, the recirculation regions increase in size and begin to cover a larger region of the channel. At the large Reynolds number, a weak recirculation region appears in wave 1 as well as other types of instabilities. These instabilities are rolling vortices that appear in the limits between the principal flow and the upper part of the recirculation.

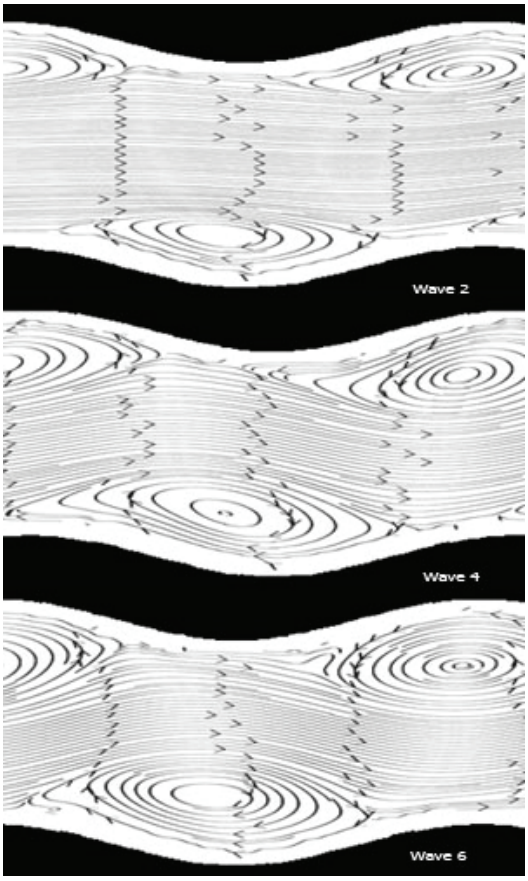

Figure 2. Pathlines; H_{avg} = 4 cm, Re = 800.

When the Reynolds number is increased the separation point moves closer to the beginning of the wave, and the reattachment point is closer to the end of the wave. In this case there are not symmetric recirculation regions, which can also be observed in Figures 2 and 3.

As the Reynolds number increases, instabilities appear in waves closer to the channel inlet. At the large Reynolds number (Re ≈ 800), some waves present random particle paths that promote macroscopic mixing over all the separation between the plates. It was observed that the wave number from inlet where macroscopic mixing first occurs, decreases as the Reynolds number increases. Macroscopic mixing was rarely observed in wave 1, even at large Reynolds numbers. For large H_{avg}, it becomes difficult

for macroscopic mixing to appear even in waves relatively far from the inlet.

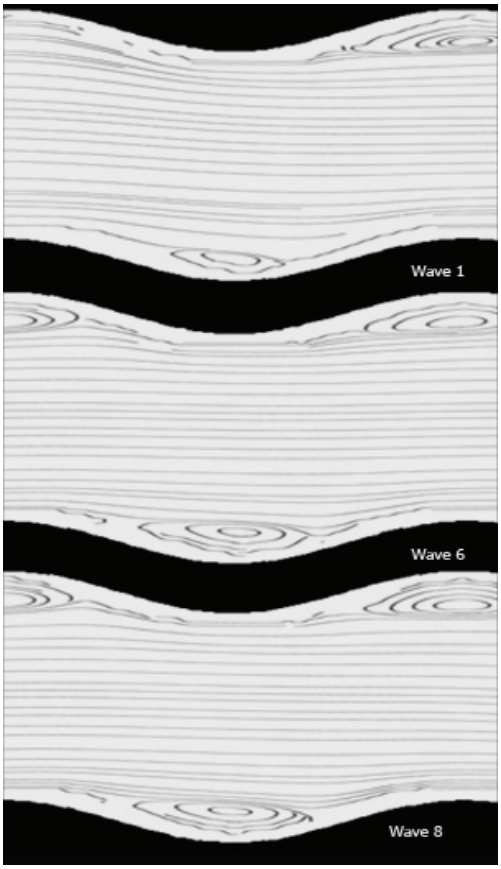

Figure 3. Pathlines; H_{avg} = 4 cm, Re = 400.

In the limits between the principal flow and the upper part of the recirculation region, rolling vortices appear. The vortices appear at the beginning of the wave and move downstream to the end of the wave, where they join the main core flow. When there are waves in the channel with macroscopic mixing, there are always waves with rolling vortices upstream from this wave. However, it is not necessarily true that macroscopic mixing exists when rolling vortices exist. It is believed that instabilities in the central flow are created by rolling vortices and flow asymmetry. Finally, it is important to mention that rolling vortices and macroscopic mixing move closer to the channel inlet as the Reynolds number increases.

In addition to the appearance of macroscopic mixing, which is also always followed by rolling vortices in downstream direction, it can be inferred that rolling vortices instabilities appear at lower Reynolds numbers than macroscopic mixing instabilities. This behavior is independent of H_{avg} (Figure 4; Tables 1 and 2).

Table 1 shows, for a range of the Re number, the closest wave number from the inlet, in which rolling vortices appear compared to experimental data found in literature [1].

The data in Table 1 shows that the increase of the average separation between plates promotes rolling vortices to appear at larger Reynolds numbers. For example, with H_{avg} = 5 cm and Re = 800 there is already a rolling vortex in wave 4, but there is a rolling vortex in wave 2 for H_{avg} = 4 cm and Re = 800. This indicates that increasing the average separation between plates makes the flow pattern in the channel steadier. Decreasing the average separation between plates promotes macroscopic mixing to appear at

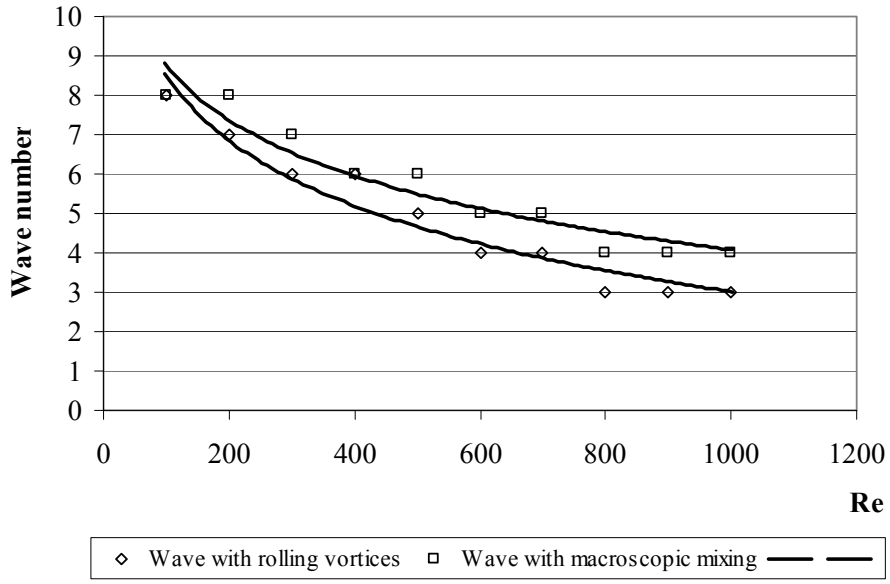

Figure 4. Comparison of the position of the first wave that presents the position of the rolling vortices and the position of the first wave that represents macroscopic mixing, H_{avg} = 5 cm.

lower Reynolds numbers; this behavior is similar to those of rolling vortices.

Table 1. Number of wave with rolling vortices counted from the inlet - comparison of the experimental data from the literature [1] and simulation data

Re	Wave number, H_{avg} / cm					
	3	4	5	3	4	5
	Experimental data			Simulation data		
200	6	8	-	6	7	8
300	5	7	8	4	6	7
400	3	6	7	3	4	6
500	2	4	6	3	4	5
600	2	3	4	2	3	4
700	2	3	4	2	3	4
800	2	3	4	2	3	3
900	2	2	3	2	2	3
1000	2	2	3	2	2	3

Table 2. Number of wave with macroscopic mixing counted from the inlet - comparison of the experimental data from the literature [1] and simulation data

Re	Wave number, H_{avg} / cm					
	3	4	5	3	4	5
	Experimental data			Simulation data		
200	8	8	8	7	7	8
300	7	7	7	7	7	7
400	6	5	7	7	6	7
500	5	5	7	5	6	6
600	5	4	6	5	5	6
700	4	3	6	4	4	6
800	3	3	6	4	4	6
900	3	3	6	3	3	6
1000	3	3	6	3	3	6

It can be seen that not only the visualized flow pattern, but also the number of wave where the rolling vortices first appear at given Re number is in a good agreement with previous investigations. For H_{avg}= 3 cm first wave in which rolling vortices appear differs for Re 300 and 500. For Re 300 in simulation data rolling vortices appear in wave number 4, while experimental data shows that they appear in wave number 5. When Re is 500 there is an opposite behavior, experimental data shows appearance of rolling vortices in wave number 2, while simulation results show that it appears in the next wave, number 3. Situation is quite similar for H_{avg} = 4 cm and H_{avg} = 5 cm. For Re values up to 500 there are slight variations of first appearance of rolling vortices. Simulations results compared to experimental data in some cases show that they appear one wave before or one wave after. For Re values from 500 to 1000 wave numbers are identical.

The closest wave number from the inlet that presents macroscopic mixing can be observed in Table 2, as a function of Re number for simulation data and experimental data found in literature [1].

The data in Table 2 shows that wave 6 presents macroscopic mixing up to Re = 800 and H_{avg} = 5 cm, while wave 4 at H_{avg} = 4 cm already has macroscopic mixing at Re = 800. This proves that increase of H_{avg} makes it more difficult for the macroscopic mixing to appear.

Simulations results compared are in a very good agreement with experimental data from the literature. For lower Re values in some cases there are differences, like for H_{avg} = 3 cm and Re = 200, the first wave with macroscopic mixing according to experimental data is wave number 8, while simulations results show that it is wave number 7. For Re values from 600 to 1000 results are almost identical. There is difference for H_{avg} = 4 cm and Re values 700 and 800, where simulation shows that the first wave is wave number 4, but experimental results show that the first wave with macroscopic mixing is wave number 3 [18].

CONCLUSIONS

The visualized flow pattern for given geometry of the heat exchanger agrees well with previous numerical and experimental investigations, which showed that the application of lattice Boltzmann method is successful in range of low Re values.

It is known that macroscopic mixing is an effective way to enhance the heat transfer and mixing in sinusoidal plates because of its random particle trajectories and although it is in some ways an interesting phenomenon - capable of improving the heat transfer and the stirring in sinusoidal plates, it does not appear in waves very near the channel inlet at the small Reynolds number range.

Previous investigations showed that enhancement of fluid mixing and formation of recirculation regions improves heat transfer. However, additional investigation on the heat transfer should be performed in order to obtain more information about the influence of recirculation regions, vortex formation, and chaotic mixing on the heat transfer enhancement.

Acknowledgement

This research was financially supported by the Ministry of Education, Science and Technological Development of the Republic of Serbia (Project No. 46010).

REFERENCES

[1] B. Giron-Palomares, A. Hernadez-Guerrero, R. Romero-Mendez, F. Oviedo-Tolentino, Int. J. Heat Fluid Flow **30** (2009) 158-171

[2] P. Gschwind, A. Regele, V. Kottke, Exp. Therm. Fluid Sci. **11** (1995) 270-275

[3] Y. Islamoglu, C. Parmaksizoglu, Appl. Therm. Eng. **24** (2004) 141-147

[4] J.Y. Jang, L.K. Chen, Int. J. Heat Mass Transfer **40** (1997) 3981-3990

[5] S. Mahmud, A.K.M.S. Islam, M.A.H. Mamun, Int. J. Eng. Sci. **40** (2002) 1495-1509

[6] T.A. Rush, T.A. Newell, A.M. Jacobi, Int. J. Heat Mass Transfer **42** (1999) 1541-1553

[7] R. Sawyers, M. Sen, C. Hsueh-Chia, Int. J. Heat Mass Transfer **41** (1998) 3559-3573

[8] J. Hardy, O. de Pazzis, Y. Pomeau, Phys. Rev. (1976) 4320-4327

[9] U. Frisch, B. Hasslacher, Y. Pomeau, Phys. Rev. Lett. (1986) 1505-1508

[10] F.J. Higuera, J. Jimenez, Europhys. Lett. **9** (1989) 663--668

[11] Y.H. Qian, D. d'Humieres, P. Lallemand, Europhys. Lett. **17** (1992) 470-484

[12] H. Chen, S. Chen, W.H. Matthaeus, Phys. Rev., A **45** (1992) 5339-5542

[13] S. Chen, G.D. Doolen, Annu. Rev. Fluid Mech. **30** (1998) 329-364

[14] Y.H. Qian, S.A. Orszag, Europhys. Lett. **21** (1993) 255--259

[15] P.H. Kao, R.J. Yang, J. Comp. Phys. 227 (2008) 5671--5690

[16] J. Latt, J.M. Krause, OpenLB User Guide, available from: http://www.openlb.org/

[17] C.C. Wang, C.K. Chen, Int. J. Heat Mass Transfer **45** (2002) 2587-2595

[18] J. Markovic, N. Lukic, D. Jovicevic, APTEFF **41** (2010) 1-203.

JELENA Đ. MARKOVIĆ
NATAŠA LJ. LUKIĆ
ALEKSANDAR I. JOKIĆ
BOJANA B. IKONIĆ
JELENA D. ILIĆ
BRANISLAVA G. NIKOLOVSKI

Univerzitet u Novom Sadu, Tehnološki fakultet, Novi Sad, Srbija

NAUČNI RAD

2D SIMULACIJA I ANALIZA STRUJANJA FLUIDA IZMEĐU DVE PARALELNE SINUSOIDALNE PLOČE PRIMENOM *LATTICE* BOLTZMANN METODE

U cilju postizanja boljeg prenosa toplote, neophodno je poboljšati mešanje fluida u razmenjivačima toplote. S obzirom na to da postoje negativni efekti pri radu razmenjivača toplote u turbulentnom režimu (kao što su značajni pad pritiska i potreba za većom pumpom) moraju se primeniti tehnike koje će obezbediti bolje mešanje fluida pri radu razmenjivača toplote u laminarnom režimu. Istraživanja su pokazala da upotreba sinusodialnih umesto ravnih ploča daje upravo ovakav rezultat. U radu su predstavljeni rezultati dvodimenzione simulacije strujanja fluida između dve paralelne sinusoidalne ploče. Simulacija je rađena modifikacijom OpenlB koda, na bazi lattice Boltzmann metode. Rejnoldsov broj prilikom simulacije je variran od 200 do 1000, a razmak između ploča od 3 do 5 cm. Rezultati pokazuju poboljšano mešanje fluida, naoročito pri većim vrednostima Rejnodsovog broja, što je u skladu sa prethodnim istraživanjima.

Ključne reči: lattice Boltzmann metod, strujanje fluida, sinusoidalne ploče, pločasti razmenjivači, simulacija.